sideband noise figure using our $0{\cdot}15 \times 40\,\mu m^2$ T-gate lattice-matched HEMT at 3dBm LO drive and 2·5mW DC power. These results are shown in Fig. 4. This is the first reported mixer with conversion gain at W band.

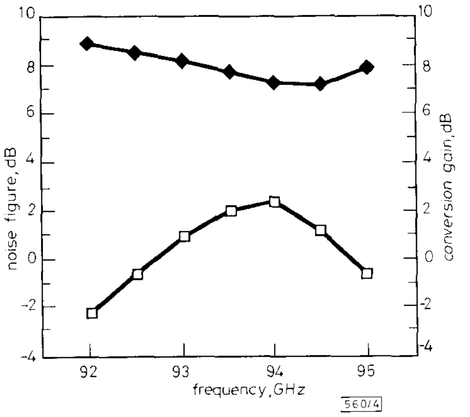


**Fig. 4** *Measured mixer conversion gain and noise figure as function of frequency*

◆ noise figure
□ conversion gain

This excellent mixer performance is due to the high device cutoff frequency as well as sharp device turn-on characteristics. The 2·4dB conversion gain achieved at W band is the result of the extremely high device cutoff frequency of 200GHz. Previous reported results for a monolithic W-band mixer using lattice matched InGaAs HEMTs with a cutoff frequency of 100GHz had a conversion loss of 13·5dB with −6·0dBm LO drive.[7] The low LO drive requirement of 3dBm reported here is the result of the extremely sharp turn-on characteristics of these devices.

In conclusion, we have fabricated $0{\cdot}15\,\mu m$ T-gate lattice-matched InAlAs/InGaAs/InP HEMTs with state of the art W-band performance. We have measured a device minimum noise figure of 1·7dB with 7·7dB associated gain. A maximum $f_T$ of 200GHz was obtained, and the 12·2dB small signal gain measured at 94GHz yielded an extrapolated $f_{max}$ of 380GHz. A single-ended active mixer was fabricated, and demonstrated the first reported conversion gain at W band.


D.C. STREIT
K. L. TAN
R. M. DIA
A. C. HAN
P. H. LIU
H. C. YEN
P. D. CHOW

*TRW Electronics and Technology Division*
*Redondo Beach, CA 90278, USA*


*9th April 1991*

## References


1 MISHRA, U. K., BROWN, A. S., ROSENBAUM, S. E., HOOPER, C. E., PIERCE, M. W., DELANEY, M. J., VAUGH, S., and WHITE, K.: 'Microwave performance of AlInAs-GaInAs HEMTs with 0·2- and $0{\cdot}1\text{-}\mu m$ gate length', *IEEE Electron Dev. Lett.*, 1988, **EDL-9**, pp. 647–649

2 DUH, K. H. G., CHAO, P. C., HO, P., TESSMER, A., LIU, S. M. J., KAO, M. Y., SMITH, P. M., and BALLINGALL, J. M.: 'W-Band InGaAs HEMT low noise amplifiers', *IEEE MTT-S Symp. Dig.*, 1990, pp. 595–598

3 CHAO, P. C., TESSMER, A. J., DUH, K. H. G., HO, P., KAO, M. Y., SMITH, P. M., BALLINGALL, J. M., LIU, S. M. J., and JABRA, A. A.: 'W-Band low-noise InAlAs/InGaAs lattice-matched HEMTs', *IEEE Electron. Dev. Lett.*, 1990, **EDL-11**, pp. 59–62

4 RIAZIAT, M., PAO, Y. C., NISHIMOTO, C., ZDASIUK, G., BANDY, S., and WENG, S. L.: 'HEMT millimetre wave monolithic amplifier on InP', *Electron. Lett.*, 1989, **25**, pp. 1328–1329

5 MAJIDI-AHY, R., RIAZAT, M., NISHIMOTO, C., GLENN, M., SILVERMAN, S., WENG, S., PAO, Y. C., ZDASIUK, G., BANDY, S., and TAN, Z.: '94GHz InP MMIC five-section distributed amplifier', *Electron. Lett.*, 1990, **26**, pp. 91–92

6 CHOW, P. D., GARSKE, D., VELEBIR, J., HSIEH, E., NGAN, Y. C., and YEN, H. C.: 'Design and performance of a 94GHz HEMT mixer', *IEEE MTT-S Symp. Dig.*, 1989, pp. 731–734

7 KWON, Y., PAVLIDIS, D., TUH, M., NG, G. I., and BROCK, T.: 'W-Band monolithic mixer using InGaAs/InGaAs HEMT', IEEE GaAs IC Symp. Dig., 1990, pp. 181–184


# CORRELATION BETWEEN LINEWIDTH REBROADENING AND LOW-FREQUENCY RIN ENHANCEMENT IN SEMICONDUCTOR LASERS

*Indexing terms: Semiconductor lasers, Lasers*


The observed correlation between the linewidth rebroadening and the low-frequency RIN enhancement at high operating power in nearly-singlemode semiconductor lasers is explained by using the two-mode rate equations which include both the self- and cross-saturation contributions to the nonlinear gain.


There are numerous applications which require narrow-linewidth semiconductor lasers.[1] Whereas progress has been made by using various DFB structures, the laser linewidth is often observed to rebroaden at high operating powers. Although a variety of explanations have been advanced to explain this behaviour, one mechanism which has received considerable attention lately is the influence of sidemodes on the laser linewidth.[2,3] This is caused by the linewidth rebroadening being often accompanied by a degradation in mode suppression ratio (MSR). However, a recent experiment using a DFB laser with four $\pi/4$ phase shifts revealed linewidth rebroadening even though the sidemodes remained suppressed by more than 30dB.[4] In addition, the linewidth rebroadening was found to be correlated with an enhancement of the low-frequency components of the relative-intensity noise (RIN) as the laser power was increased. This observed correlation has yet to be explained. We demonstrate that the correlation between linewidth and low-frequency RIN arises naturally from the laser rate equations. Our model, which includes the nonlinear gain effects, demonstrates that linewidth rebroadening can occur even when the MSR does not degrade with increasing power, as observed experimentally in Reference 4.

The analysis uses the four rate equations for the mainmode and sidemode photon numbers $P_1$ and $P_2$, the mainmode phase $\phi$, and the total number of electrons $N$ in the cavity.[5] The rate equations are linearised for small fluctuations from the steady-state values, and the resulting equations are solved in the Fourier domain. Because the entire procedure is well known,[6] we omit most of the details. The selfsaturation and cross-saturation effects are included through the mode gain expression written as

$$G_i = A(N - N_0) - \beta_i P_i - \theta_{ij} P_j \quad (i, j = 1, 2;\ i \neq j) \qquad (1)$$

where the subscript 1 or 2 refers to the mainmode or sidemode. Table 1 describes each parameter and gives the value used. The mainmode linewidth, approximated from the zero-frequency component of the frequency noise spectrum, is found to be given by[5]

$$\Delta\nu = \frac{R_{sp}}{4\pi P_1}\left\{1 + \alpha^2 \frac{(GAP_1)^2}{|L(0)|^2} \times \left[|H_{21}^{(2)}(0)|^2 + |H_{12}^{(1)}(0)|^2 \frac{P_2}{P_1}\right]\right\} \qquad (2)$$

where

$$L(\omega) = (\Gamma_n + i\omega)B(\omega) + GAP_1 H_{12}^{(2)}(\omega) + GAP_2 H_{21}^{(1)}(\omega) \quad (3a)$$

$$H_{km}^{(j)}(\omega) = \Gamma_j + i\omega - \theta_{km} P_j \quad (j, k, m = 1, 2; k \neq m) \quad (3b)$$

$$B(\omega) = (\Gamma_1 + i\omega)(\Gamma_2 + i\omega) - \theta_{12}\theta_{21}P_1P_2 \quad (3c)$$

$$\Gamma_j = R_{sp}/P_j + \beta_j P_j \quad (j = 1, 2) \quad (3d)$$

The expression for the RIN of the total power is found in a similar fashion to be

$$RIN(\omega) = \frac{2R_{sp}P_1(\Gamma_n^2 + \omega^2)}{(P_1 + P_2)^2 |L(\omega)|^2} \times \left[ |H_{21}^{(2)}(\omega)|^2 + |H_{12}^{(1)}(\omega)|^2 \frac{P_2}{P_1} \right] \quad (4)$$

A comparison between eqns. 2 and 4 for $\Delta\nu$ and $RIN(\omega)$ shows a striking similarity. In fact, we may write the linewidth in terms of the low-frequency part of the total $RIN$ as

$$\Delta\nu = \frac{R_{sp}}{4\pi P_1}\left\{1 + \alpha^2 (GAP_1)^2 \frac{P_T^2 RIN(\omega = 0)}{2R_{sp}P_1\Gamma_n^2}\right\} \quad (5)$$

where $P_T = P_1 + P_2$ is the total photon number. Eqn. 5 demonstrates that the correlation between the linewidth rebroadening and the low-frequency $RIN$ enhancement is actually predicted by the laser rate equations.

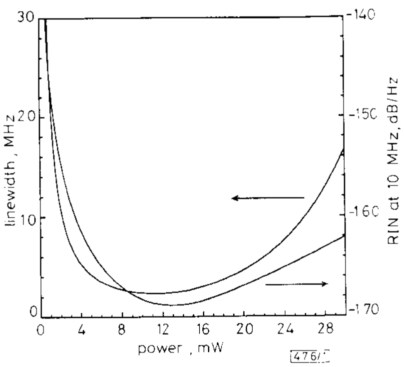


**Fig. 1** *Correlation rebroadening of linewidth and total RIN as laser power is increased*

Using the parameter values in Table 1 with $\beta_1 = \beta_2 = \beta$ and $\theta_{12} = \theta_{21} = \theta$, we illustrate this result in Fig. 1 by plotting linewidth and low-frequency $RIN$ as a function of total output power. As the laser power is increased beyond 10 mW, both linewidth and the low frequency $RIN$ start to increase. This is similar to the experimental results of Reference 4. We stress that it is the total $RIN$ and not the mainmode $RIN$ which is being plotted in Fig. 1. It is well known that mode partition noise leads to an enhancement in the low-frequency $RIN$ of the mainmode; this enhancement is caused by carrier-induced mode competition. The total $RIN$, however, remains low because of the anticorrelation between the two modes. In the present model, nonlinear gain generates additional mode coupling over and above the mode-partition effects. Such coupling, in the form of cross-saturation by the sidemode power, causes larger low-frequency fluctuations even in the total power. To demonstrate this effect, we plot in Fig. 2 the total RIN against frequency for three different operating powers. As the power is increased, the total $RIN$ is enhanced in the low frequency regime ($<1$ GHz) by more than 10 dB relative to the singlemode value.[7]

From a device standpoint, the power level at which the linewidth rebroadening begins is a very important quantity. To estimate this quantity, and simultaneously to provide a physical explanation for the main features of Fig. 1, we look more closely at eqn. 2 and consider different limiting cases. Using eqn. 3$b$, $\Delta\nu$ may be written as

$$\Delta\nu = \frac{R_{sp}}{4\pi P_1}\left\{1 + \alpha^2 \frac{(GAP_1)^2}{|L(0)|^2} \times \left[(\Gamma_2 - \theta P_2)^2 + (\Gamma_1 - \theta P_1)^2 \frac{P_2}{P_1}\right]\right\} \quad (6)$$

The second term in the brackets which is proportional to $P_2/P_1$ arises from carrier-induced mode coupling. The mode coupling through nonlinear gain is expressed through the

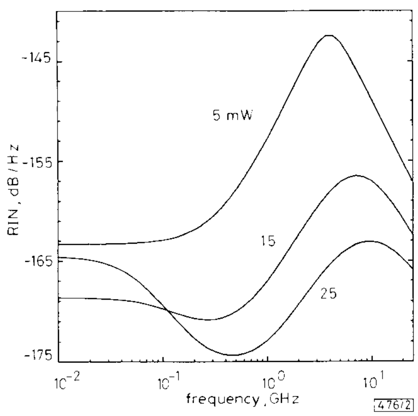


**Fig. 2** *Total RIN against frequency for three different output powers showing low-frequency enhancement at higher operating powers*

parameter $\theta$. The mainmode and sidemode fluctuation damping rates $\Gamma_1$ and $\Gamma_2$ follow quite different behaviour as the total power increases for a constant MSR. The reason is that $\Gamma_2$ is dominated by spontaneous emission ($\Gamma_2 \simeq R_{sp}/P_2$) whereas $\Gamma_1$ is dominated by nonlinear gain ($\Gamma_1 \simeq \beta P_1$). At low output power, the $P_2/P_1$ term is negligible because $\Gamma_2$ is very large; furthermore, $[L(0)]^2 \simeq [GAP_1(\Gamma_2 - \theta P_2)]^2$ so that the linewidth reduces to the familiar singlemode result: $\Delta\nu = (R_{sp}/4\pi P_1)(1 + \alpha^2)$. As the output power increases, $\Gamma_2$ becomes smaller while $\Gamma_1$ grows larger, and the two bracketed terms in eqn. 6 can become comparable even though $P_2/P_1$ is very small. By equating these two terms and using eqn. 3$d$, the power level at which rebroadening occurs thus may be written approximately as

$$P_R \simeq K^{-1}\sqrt{\left(\frac{R_{sp}}{|\beta - \theta|}\right)} MSR^{3/4} \quad (7)$$

where $K$ is a constant used to convert photon number to milliwatts. Using the values in Table 1, this corresponds to about 14 mW, which agrees well with Fig. 1. As the power is increased further, the theory predicts the linewidth to reach a maximum and again to decrease with power. This happens even without cross-saturation ($\theta = 0$), in which case the linewidth rebroadens by about 10 MHz and then begins to

**Table 1** TYPICAL VALUES FOR MULTIPLE QUARTER-WAVE SHIFTED *DFB* LASER WITH 3% REFLECTING FACETS, 40 cm$^{-1}$ OF INTERNAL LOSS, AND ACTIVE REGION DIMENSIONS OF $2 \times 0{\cdot}2 \times 900\,\mu m^3$

| | | |
|---|---|---|
| $A$ | Linear gain coefficient | $1875\,s^{-1}$ |
| $N_0$ | Electron transparency number | $3{\cdot}6 \times 10^8$ |
| $\beta_i$ | Self-saturation coefficient of mode $i$ | $5 \times 10^4\,s^{-1}$ |
| $\theta_{ij}$ | Cross-saturation coefficient ($i \neq j$) | $6{\cdot}7 \times 10^4\,s^{-1}$ |
| $R_{sp}$ | Spontaneous emission rate in both modes | $1{\cdot}3 \times 10^{12}\,s^{-1}$ |
| $\alpha$ | Linewidth-enhancement factor | 5 |
| $\Gamma_n$ | Decay rate of electron number fluctuations | $2{\cdot}2 \times 10^9\,s^{-1}$ |
| $\Gamma_i$ | Decay rate of fluctuations in mode $i$ | see eqn. 3$d$ |
| $MSR$ | Mode-suppression ratio ($P_1/P_2$) | 30 dB |
| $G$ | Steady-state mode gain | $6{\cdot}2 \times 10^{11}\,s^{-1}$ |
| $K$ | Number of photons in 1 mW of power | $1{\cdot}07 \times 10^5$ |

decrease. However, the enhancement in the low-frequency *RIN* which occurs in the absence of cross-saturation is only a few dB and would be too small to explain the experimental results shown in Reference 4. On the other hand, by including the cross-saturation effects with $\theta > \beta$, both low-frequency *RIN* and linewidth peak sharply at a particular output power level. This critical power level $P_C$ is that which minimises $L(0)$ and may be written as

$$P_C \simeq K^{-1} \sqrt{\left(\frac{R_{sp}}{2(\theta - \beta)}\right)} MSR \tag{8}$$

Using the values in Table 1, this corresponds to a power level of 58 mW at which linewidth and low-frequency *RIN* peak as a function of output power.

This analysis has been performed for a constant value of *MSR*; i.e. the *MSR* does not degrade with increasing power. Rather, as the total power is increased, the side mode power also increases. Note that the expressions for the power levels at which rebroadening begins $P_R$ and reaches a peak $P_C$ depend upon *MSR*. As the *MSR* is improved, the rebroadening is pushed to higher powers and thus may not always be observable. Although we have expressed the linewidth turning points in terms of output power ($P_R$ and $P_C$), the key parameter is actually the sidemode power. Because a quarter-wave shifted laser stores more photons per mW in the cavity, the sidemode power can be larger than in a conventional laser operating at the same *MSR*.

To summarise, we have shown that the experimentally-observed correlation between the linewidth rebroadening and the low-frequency *RIN* enhancement arises naturally from the rate equations. Without degradation of the *MSR*, the linewidth rebroadens with increasing output power due to carrier-induced mode coupling. The effect of cross-saturation by the sidemode leads to a maximum increase in the laser linewidth and the low-frequency total *RIN*. Both begin to decrease monotonically at still higher output power.

*Acknowledgments:* This research is supported by the US Army Research Office and the Joint Services Optics Program.

G. R. GRAY
G. P. AGRAWAL

*The Institute of Optics*
*University of Rochester*
*Rochester, NY 14627, USA*

*27th March 1991*

**References**

1 KOCH, T. L., and KOREN, U.: 'Semiconductor lasers for coherent optical fiber communications', *J. Lightwave Technol.*, 1990, **8**, pp. 274–293

2 KRUGER, U., and PETERMANN, K.: 'Dependence of the linewidth of a semiconductor laser on the mode distribution', *IEEE J. Quantum Electron.*, 1990, **QE-26**, pp. 2058–2064

3 MILLER, S. E.: 'The influence of power level on injection laser linewidth and intensity fluctuations including side-mode contributions', *IEEE J. Quantum Electron.*, 1988, **QE-24**, pp. 1873–1876

4 SUNDARESAN, H., and FLETCHER, N. C.: 'Correlation of relative intensity noise with linewidth floors in narrow linewidth DFB lasers', *Electron. Lett.*, 1990, **26**, pp. 2002–2003

5 GRAY, G. R., and AGRAWAL, G. P.: 'Effect of cross saturation on frequency fluctuations in a nearly-single-mode semiconductor laser', to be published in *IEEE Photonics Technol. Lett.*, 1991, **3**

6 AGRAWAL, G. P.: 'Mode-partition noise and intensity correlation in a two-mode semiconductor laser', *Phys. Rev. A*, 1988, **A37**, pp. 2488–2494

7 SU, C. B., SCHLAFER, J., and LAUER, R. B.: 'Explanation of low-frequency relative intensity noise in semiconductor lasers', *Appl. Phys. Lett.*, 1990, **57**, pp. 849–851

## NEW MEASUREMENT TECHNIQUE FOR WAVEGUIDE LOSSES BASED ON PHOTOLUMINESCENCE

*Indexing terms: Waveguides, Losses, Measurement, Photoluminescence*

A new technique has been developed to measure optical losses of waveguide devices fabricated in III-V semiconductors by optical excitation of an integrated twinguide structure, which is nondestructive and also applicable to multimode waveguides and multiport waveguide devices. Reproducibility of excitation was found to be better than 0·2 dB.

*Introduction:* As OEICs are expected to play an important role in future telecommunication systems there is an increasing demand for accurate techniques for measuring the transmission losses of waveguide devices fabricated in III-V semiconductors. Until recently the cutback method was widely applied to this type of measurement. In our laboratory it has been applied for determining the losses of straight and bent InGaAsP waveguides.[1]

A disadvantage of this method is its destructive character. A quick and accurate nondestructive method, which has become increasingly popular, is the Fabry–Perot method.[2] This method is, however, restricted to singlemode two-port devices. We present a nondestructive measurement technique which is applicable to multiport devices with single or multimode waveguides.

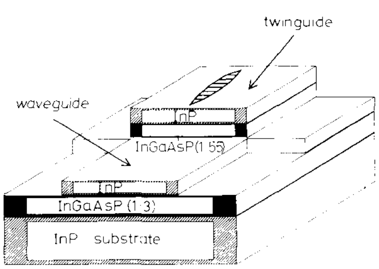


**Fig. 1** *Schematic representation of integrated twinguide structure*

*Principle:* The method is based on optical pumping of an integrated twinguide structure[3] (see Fig. 1). The twinguide consists of a low-bandgap layer [InGaAsP(1.55)] on top of the waveguide layer [InGaAsP(1.3)], separated by a thin InP etch-stop layer. Part of the photoluminescence of the upper quaternary layer ($\lambda = 1{\cdot}55\,\mu$m) will be trapped in the twinguide and propagate in the form of twinguide modes. At the transition between the twinguide and the waveguide section a substantial part of this light is coupled into the transparent waveguide. The light emanating from the waveguide is imaged onto a photodiode. Waveguide attenuation can be measured by fabricating a number of twinguide blocks at different distances from the cleaved edge (Fig. 2). Component losses are measured by comparing the output power with that of a straight waveguide.

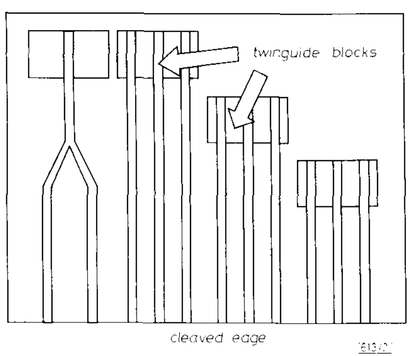


**Fig. 2** *Fabrication of twinguides at different distances from cleaved edge allowing determination of waveguide losses*